processes

MDPI

Article

Development of an Innovative and Sustainable Technological Process for Biogas Purification Through the Reuse of Autoclaved Aerated Concrete Waste

Eric Dumont [1,*], Noé Kautzmann [2] and Annabelle Couvert [2]

[1] Nantes Université, IMT Atlantique, CNRS, GEPEA, UMR 6144, F-44000 Nantes, France
[2] Université de Rennes, Ecole Nationale Supérieure de Chimie de Rennes, CNRS, ISCR, UMR 6226, F-35000 Rennes, France; noekautzmann@gmail.com (N.K.); annabelle.couvert@ensc-rennes.fr (A.C.)
* Correspondence: eric.dumont@imt-atlantique.fr

Abstract: This study demonstrated the effectiveness of using autoclaved aerated concrete AAC waste as a low-cost filtering material for removing hydrogen sulfide (H_2S) from gas streams. A long-term experiment (89 days) was conducted in a packed bed reactor to purify synthetic biogas composed of N_2, CO_2, H_2S, and O_2. Optimal H_2S removal efficiencies, reaching up to 100%, were achieved under highly acidic conditions (pH ≈ 1–3) and low oxygen concentrations (<1%). In the presence of oxygen, calcium oxides in the AAC waste react with H_2S to form gypsum ($CaSO_4$ $2H_2O$). The simultaneous removal of both oxygen and H_2S by AAC waste, following an approximate 2:1 molar ratio, may be particularly beneficial for biogas streams containing unwanted traces of oxygen. The transformation and lifespan of AAC waste were monitored through sulfur accumulation in the material and pressure drop measurements, which indicated structural changes in the AAC waste. At the end of its lifespan, the AAC waste exhibited an H_2S removal capacity of 185 g_{H_2S} $kg_{AAC}{}^{-1}$. This innovative and sustainable process not only provides a cost-effective and environmentally sound solution for the simultaneous removal of H_2S and O_2 from biogas, but also promotes waste valorization and aligns with circular economy principles.

Keywords: H_2S; biogas; purification; autoclaved aerated concrete; recycling; circular economy

check for updates

Academic Editor: Marco Race

Received: 6 May 2025
Revised: 27 May 2025
Accepted: 30 May 2025
Published: 3 June 2025

Citation: Dumont, E.; Kautzmann, N.; Couvert, A. Development of an Innovative and Sustainable Technological Process for Biogas Purification Through the Reuse of Autoclaved Aerated Concrete Waste. *Processes* **2025**, *13*, 1767. https://doi.org/10.3390/pr13061767

Copyright: © 2025 by the authors. Licensee MDPI, Basel, Switzerland. This article is an open access article distributed under the terms and conditions of the Creative Commons Attribution (CC BY) license (https://creativecommons.org/licenses/by/4.0/).

1. Introduction

On a global scale, it is estimated that more than 4.8 billion tons of concrete waste from construction and demolition will be produced annually by 2030 [1]. Therefore, efforts must be made to continue developing innovative sustainable technologies for recovering this waste to reduce the carbon footprint of concrete [2,3]. Among the wide variety of concrete waste, this study focuses on autoclaved aerated concrete (AAC), also known as cellular concrete. It is a lightweight building material with excellent thermal insulation and fire-resistant properties. It is composed of silica sand, cement, calcium oxides, water, and aluminum powder, which acts as an expansion agent. The main recycling options for AAC waste, aimed at avoiding landfilling, are related to the building industry. These include the production of new AAC, light mortar, lightweight aggregate concrete, and shuttering blocks made from concrete without fine fractions [4]. But recycling alternatives do exist, particularly in the field of gas purification, notably for gases laden with hydrogen sulfide (H_2S) [5]. Hydrogen sulfide is a toxic and corrosive gas commonly encountered in

various industrial and natural environments, including gas processing facilities, wastewater treatment plants, landfills, and anaerobic digesters used in biogas production. Given the increasing role of biogas as a renewable energy source (biogas is a mixture composed primarily of methane (CH_4) and carbon dioxide (CO_2), along with trace components such as nitrogen (N_2), oxygen (O_2), ammonia (NH_3), and H_2S [6]), ensuring its clean utilization is critical to supporting environmental sustainability and climate change mitigation efforts [7]. Current technologies for H_2S removal from biogas include physicochemical techniques (membrane separation, absorption, cryogenic distillation, advanced oxidation processes, adsorption) as well as biological techniques (biofilters, biotrickling filters, and bioscrubbers) [8,9]. The predominant techniques are absorption, which involves the use of a scrubbing solution (alkanolamines, ionic liquids, deep eutectic solvents, or hybrid blends), and adsorption, which involves packed columns containing sorbents such as activated carbons, zeolites, and/or metal oxides. In terms of H_2S separation capacity, some activated carbons outperform other materials such as biochars, zeolites, metal-organic frameworks (MOFs), and metal-based adsorbents [9]. However, to be efficient, these activated carbons must be functionalized by impregnation or metal loading, which significantly increases cost. It is also important to consider the effects of water and oxygen (O_2), both of which can have an impact on H_2S separation. Moreover, powdered activated carbon can cause substantial pressure drops, which increases energy consumption due to additional gas compression. Regeneration of these sorbents can pose difficulties and reduce their adsorption capacity. Furthermore, the elimination of non-regenerable sorbents poses an environmental risk due to the formation of sulfuric acid (H_2SO_4), an oxidation product of the H_2S separation process. These limitations underscore the need for innovative, cost-effective, and sustainable materials that align with circular economy principles. Interestingly, the natural degradation of concrete observed in sewer systems and wastewater treatment infrastructure, caused by sulfuric acid generated from microbial activity [10–12], can inspire new pollutant removal technologies. Preliminary studies in our laboratory have demonstrated that humidified fixed beds of AAC waste can act as an efficient, low-cost, and robust purification system for H_2S-laden gases [13–15]. The removal mechanism involves complex physico-chemical interactions with AAC constituents, particularly calcium and ferric oxides. Given the abundant availability of AAC waste, this simple technology could offer a sustainable pathway for biogas purification. The use of AAC waste for H_2S removal in biogas is a novel area of research. To our knowledge, no data currently exist in the literature, aside from our results, that allow for direct comparison with other adsorbent materials. But a recent biogas biofiltration study using cellular concrete waste as a packing material enriched with sulfur-oxidizing bacteria (*Thiobacillus*) reported an elimination capacity (EC) of 100 $g_{H_2S}\ m^{-3}\ h^{-1}$ and a moderate removal efficiency (RE) of 75% [16]. However, the authors did not address the influence of oxygen, which is a critical factor in both the biofiltration process and the physical H_2S removal by AAC waste presented in the present study.

Our initial laboratory studies were carried out using a synthetic gas mixture composed of nitrogen (in place of methane for safety reasons), H_2S, and uncontrolled traces of oxygen. The presence of O_2 appeared to influence the removal performance, although it could not be precisely quantified [14]. Other parameters, such as CO_2 concentration and pH effects, were not considered. Therefore, the present experimental work was undertaken using synthetic gas mixtures more representative of actual biogas, with controlled levels of N_2, CO_2, O_2, and H_2S. The objective was to investigate the influence of O_2 and CO_2 on H_2S removal efficiency, and to determine the reaction stoichiometry, including the ratios of H_2S removed to O_2 consumed and to CO_2 consumed or produced. The impact of pH on these reactions was also examined.

2. Materials and Methods

2.1. Material

The autoclaved aerated concrete used in this study was provided by Ecominero, a French eco-organization dedicated to managing waste from construction, demolition, and excavation activities (https://www.ecominero.fr/, accessed on 29 May 2025). Before being introduced as a packing material in the PBR, the AAC waste was sieved to isolate pieces approximately 10–15 mm in diameter (Figure 1). The elemental composition of AAC was determined using an Energy Dispersive X-ray Fluorescence Spectrometer (EDX-800HS, Shimadzu Company, Kyoto, Japan). Prior to contact with H_2S-laden gas, the AAC waste was primarily composed (by weight) of SiO_2 (50.5%), CaO (24.6%), SO_3 (19.7%), Al_2O_3 (2.2%), P_2O_5 (1.4%), and Fe_2O_3 (1.3%). These data agree with those reported by [13]. A complementary analysis was carried out using X-ray Diffraction (XRD) (Siemens Brüker D5000, Karlsruhe, Germany). The following phases were identified: quartz (SiO_2), calcium carbonate ($CaCO_3$), gypsum ($CaSO_4$, $2H_2O$), aluminum oxide (Al_2O_3), iron oxide (Fe_2O_3), and calcium silicate hydroxide hydrate ($Ca_{45}Si_6O_{15}(OH)_3$, $2H_2O$). Specific surface area was determined using a Micromeritics ASAP® 2020 gas adsorption analyzer (Micromeritics Company, Norcross, GA, USA). The specific surface area (44 ± 0.8 m^2 g^{-1}) was calculated by the Brunauer-Emmett-Teller (BET) method. Internal porosity (64%) and apparent density (547 kg m^{-3}) were measured using a mercury porosimeter, Micrometrics autopore IV 9500 (Micromeritics Company, Norcross, GA, USA). The water retention capacity of AAC waste, defined as the maximum mass of water retained per gram of dry material, was measured by immersing the material in water for 1 h, followed by draining for 24 h. The increase in mass was used to calculate the water retention, which was found to be $56 \pm 2\%$. The pH of AAC waste was measured at 9 using a pH electrode connected to a Consort C561 multi-parameter analyzer (Consort, Turnhout, Belgium). A CHNS elemental analyzer (Carbon, Hydrogen, Nitrogen, Sulfur, Flash EA Series 1112, Thermo Scientific, Waltham, MA, USA) was also used to quantitatively determine the variation in sulfur content in the material between the beginning and the end of the experiment. The composition of AAC waste at the start of the experiment was (mass percentage): calcium Ca: 59.4%, silicon Si: 29.0%, sulfur S: 5.5%, iron Fe: 2.8%, aluminum Al: 1.2%, potassium K: 0.8%, and phosphorus P: 0.6%.

2.2. Experimental Setup

The experimental setup (Figure 1) consisted of a PVC cylindrical column (with internal diameter 100 mm), referred to as the "packed bed reactor" (PBR) in the text, filled with 7.8 L of AAC over a height of 1 m, along with a water tank. The PBR was equipped with six sampling ports located at 0, 20, 40, 60, 80, and 100 cm from the bottom for sampling, concentration determination, and pressure drop measurements. The synthetic gas in contact with the AAC was a mixture of N_2-CO_2-H_2S-O_2 simulating raw biogas. A BrezzaNiGen nitrogen generator (LCMS 40-1, with up to 99.9% purity) from Gengaz Company (Wasquehal, France) provided a continuous nitrogen supply to the PBR. The nitrogen flow rate was controlled and measured with a mass flowmeter (Model 58500, Brooks Instruments, Hatfield, PA, USA). Despite the generator's capability to purify nitrogen from air, a low fraction of uncontrolled oxygen was consistently measured in the nitrogen gas. Consequently, an air flow rate regulated by a mass flowmeter (Brooks Instruments, Hatfield, PA, USA) was added in order to adjust the O_2 concentration to the desired level in the gas entering the PBR (around 0.3%, i.e., 3000 ppm). A CO_2 flow (99.5% purity) and a H_2S flow (99.7% purity), both controlled by dedicated mass flow meters (Brooks Instruments, Hatfield, PA, USA), were also mixed into the main N_2 stream before entering the PBR. The concentrations of N_2, CO_2, H_2S, and O_2 were simultaneously measured using a gas chromatography analyzer (micro GS Fusion® gas analyser, Inficon, Bad Ragaz, Switzerland), which was alternately

connected to the six sampling ports. A sodium hydroxide (NaOH) trap, positioned after the PBR, was used to remove residual H_2S at the end of the treatment. The treated gas was then vented outside.

All experiments were carried out under humid conditions, monitored by a humidity sensor (Model EE08, E+E Electronik GmbH, Engerwitzdorf, Austria) located at the top of the PBR. To maintain optimal humidity conditions, the AAC was continuously moistened with tap water using a drip system. The water circulated in a closed loop between the top and bottom of the PBR. The relative humidity measurements of the gas at the PBR outlet consistently exceeded 97%. The gradual accumulation of sulphate (SO_4^{2-}) in the water due to H_2S oxidation was measured using a High Pressure Ion Chromatography (940 Professional IC Vario, Metrohm, Switzerland). Thermocouples (K type) were installed to measure temperatures at various levels within the PBR, and pressure drops were measured with a Setra pressure sensor (Setra Systems, Inc., Boxborough, MA, USA; 0–700 Pa).

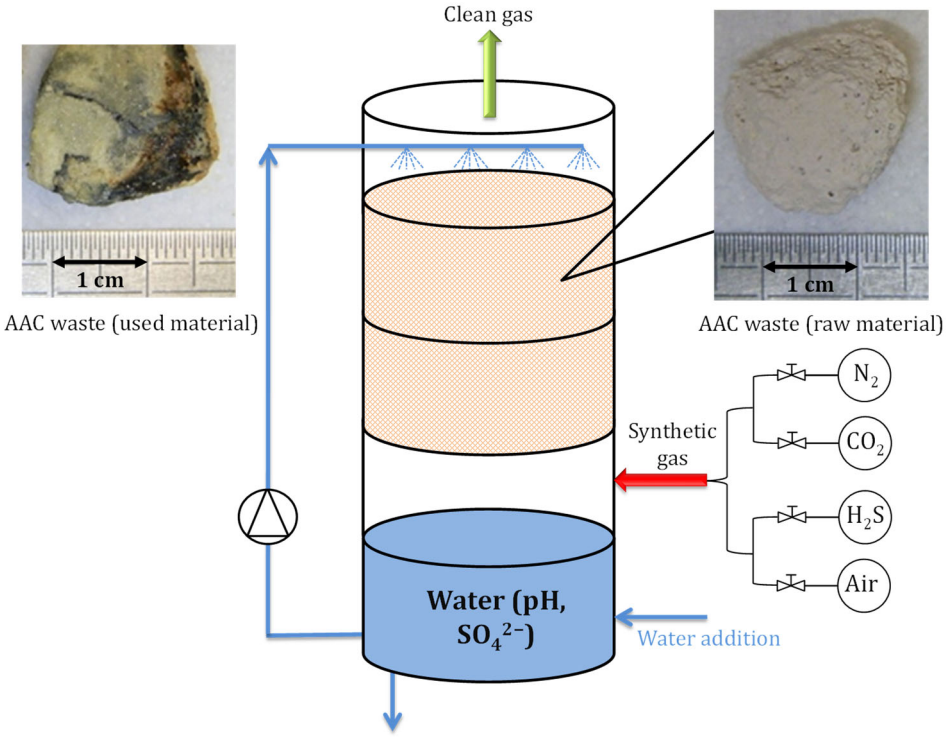


Figure 1. Sketch of the experimental setup used for the removal of H_2S, and photos of AAC waste (right: raw material at the beginning of experiment; Left: piece retrieved from the packed bed reactor (PBR) at the end of experiment).

2.3. Operating Conditions

The experiment focused on monitoring the behavior of AAC waste in contact with the loaded gas throughout the lifespan of the material, as well as determining the optimal operating conditions, particularly in terms of pH. The experiment was carried out in two distinct phases (Table 1): a transient phase (one month), during which the loading rate (LR) was progressively increased from 9.0 ± 0.5 to 72 ± 4 g_{H_2S} m^{-3} h^{-1} by raising the applied H_2S concentration and reducing the residence time, and a steady-state phase (two months) at the maximum loading rate. The loading rate refers to the mass of H_2S applied to the treatment system per unit volume of AAC in the PBR and per unit of time. At the start of the experiment, the pH of the tap water used to moisten the AAC was close to neutral.

Table 1. Operating conditions.

Transient Phase	Steady State
From days 1 to 33	From days 34 to 89
Residence time [1]: 60 ± 1 ↘ 22 ± 1 s H_2S concentration: 105 ↗ 400 ↘ 300 ± 6 ppm Loading Rate [2]: 9.0 ± 0.5 ↗ 72 ± 4 g_{H_2S} m^{-3} h^{-1} O_2 concentration: 2–3% (20,000–30,000 ± 600 ppm)	Residence time = 22 ± 1 s H_2S concentration = 300 ± 6 ppm Loading Rate = 72 ± 4 g_{H_2S} m^{-3} h^{-1} O_2 concentration: 3 ↘ 0.3% (20,000–3000 ± 60 ppm)

[1] Residence time = $volume_{AAC}$ (m^3)/gas flowrate (m^3 s^{-1}). [2] Loading rate LR = H_2S concentration (g m^{-3}) × gas flowrate (m^3 h^{-1})/$volume_{AAC}$ (m^3). Note that 1 ppm_{H_2S} = 1.4 mg m^{-3} at 25 °C and 101 kPa.

3. Results and Discussion

3.1. H_2S Removal Efficiency

The evolution of the capacity of AAC waste to remove H_2S in the experiment is shown in Figure 2 through a bar chart illustrating the removal efficiency RE = 100 × (C_{inlet} − C_{outlet})/C_{inlet}. During the transient phase, between days 1 and 25, RE decreased from 80 ± 4 % to 20±1% in relation to the increase in the loading rate from 9.0 ± 0.5 to 65 ± 4 g m^{-3} h^{-1}. The pH of the recirculating water was roughly constant around neutral, and the O_2 concentration was very high, around 2–3%, due to a malfunction in the nitrogen generator. On day 24, 6 L of acidic water (pH = 1.2 ± 0.1) was added to the water tank to improve the efficiency of the AAC waste. Consequently, the pH dropped from 7.3 ± 0.1 to 5.4 ± 0.1 before increasing to 6.6 ± 0.1, due to the alkaline nature of the material. The alkalinity of AAC waste helps neutralize the acidic byproducts generated during reactions with H_2S, in the same way that alkaline materials, such as lime, are used to enhance the efficiency of industrial gas scrubbers treating H_2S [17]. This operation proved beneficial, as the pH then steadily decreased due to the production of sulfuric acid, confirmed by the accumulation of sulphate (SO_4^{2-}) in the water. By the end of the transient phase, the pH was around 4.0 ± 0.1, and RE increased to 60 ± 3%. This result highlights the importance of performing an acid attack on the material to achieve significant treatment performance. During the steady-state phase, two different situations can be observed in Figure 2. Between days 26 and 50, RE ranged from 50 ± 3% to 65 ± 3%, whereas between days 54 and 78, the removal efficiency exceeded 95 ± 4% and occasionally reached 100%. These two situations differ in terms of oxygen concentration and pH. Between days 26 and 50, pH values were around 3.0, and the O_2 concentration was approximately 3%. In contrast, between days 54 and 78, the O_2 concentration was 10 times lower, around 0.3%, and pH values decreased from 3.0 to 1.0. Although it is difficult to draw definitive conclusions about the respective influence of these two parameters on the efficiency of H_2S elimination, it seems necessary to operate at low O_2 concentration and very acidic pH values, around 2–3 (as will be confirmed later in Section 3.5). In practical applications, pH values can be easily regulated, whereas O_2 concentration, which is typically lower than 1% in biogas, cannot be controlled. After day 81, it was observed that RE decreased significantly to 30 ± 2%, despite the fact that the pH was close to 1.0 and the O_2 concentration remained around 0.3%. This drop in RE corresponds to the end of the AAC's lifespan, meaning that the main components of the AAC capable of reacting with H_2S, i.e., calcium oxides [14], were almost entirely consumed.

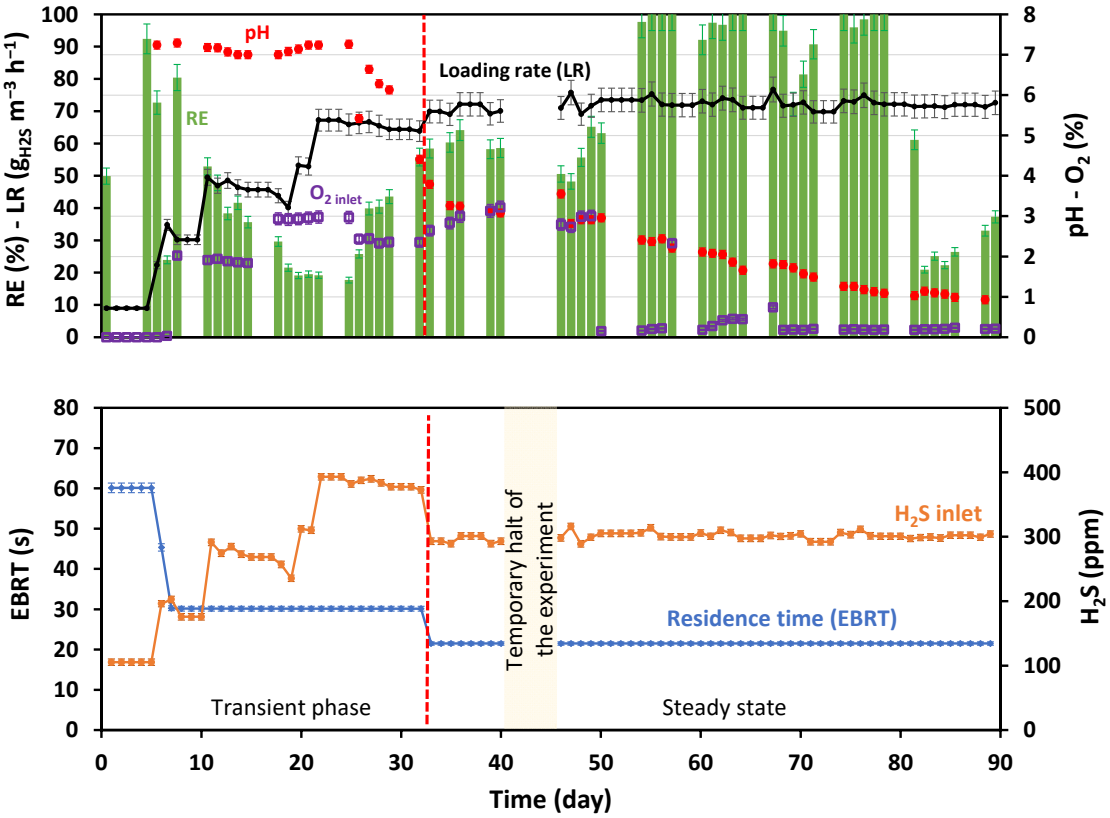


Figure 2. Influence of the applied loading rate, pH, and O_2 concentration on H_2S removal efficiency.

3.2. Pressure Drops

The physico-chemical reactions that occur between H_2S and the components of AAC waste lead to a significant change in the pressure drops (ΔP) recorded over time (Figure 3). Initially, the pressure drops across the PBR were very low (around 5.0 ± 0.3 Pa·m^{-1}), which is very favorable in terms of fan power consumption. Then, the progressive transformation of the AAC waste resulted in a moderate and linear increase in ΔP over time (up to 23 ± 2 Pa·m^{-1} on day 71), followed by a dramatic rise on day 81 (up to 60 ± 3 Pa·m^{-1}, i.e., a three-times increase). This sharp increase in ΔP, concomitant with the drop in efficiency observed in Figure 2, indicates that the nature of the AAC waste has been profoundly altered. According to Poser et al. [14], the primary reaction between H_2S and AAC waste involves the disappearance of calcium oxides ($CaO\ SiO_2 \cdot nH_2O$ and $CaCO_3$) and the formation of calcium sulfate ($CaSO_4 \cdot nH_2O$, i.e., gypsum), which represents a significant transformation of the material. After transformation, the highly moistened material obtained can be easily crushed, whereas the original AAC waste could not. The transformation of AAC waste into gypsum leads to a significant change in the pressure drops recorded over time. Consequently, this rapid increase in ΔP over a short period serves as a reliable indicator that the material's capacity to treat H_2S is nearly exhausted and that it is necessary to replace it. From an industrial perspective, monitoring this indicator, which is reliable, easy to implement, and cost-effective, represents a major advantage for controlling the H_2S purification process and the replacement of used AAC waste. Considering that the main reactive capacities with H_2S are significantly altered from day 81 onward, it can be deduced that the removal capacity of material was 185 ± 8 g_{H_2S} $kg_{AAC}{}^{-1}$ (Figure 3). However, this value does not represent the maximum, as the AAC was still capable of removing part of the H_2S with efficiencies ranging from 20 ± 1% to 30 ± 2% (Figure 2). This value is slightly higher than that reported in a previous study (169 g_{H_2S} $kg_{AAC}{}^{-1}$ by [14]) and is of the same order of magnitude as that of commercial adsorbents used for H_2S removal,

generally between 50 and 200 g_{H_2S} kg^{-1} [9,18–20]. Consequently, the use of AAC waste could represent a very promising, low-cost alternative to the use of activated carbon for H_2S removal.

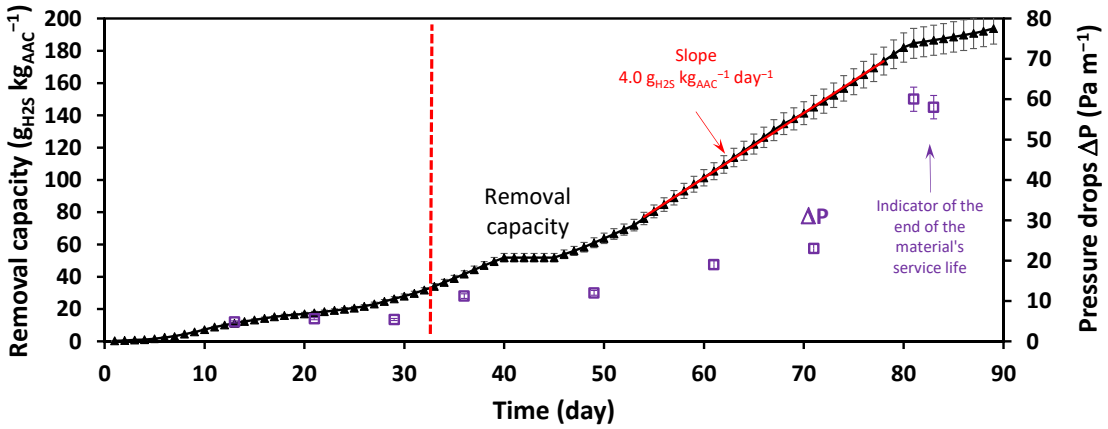


Figure 3. Cumulative amount of H_2S removed by AAC over time, and pressure drops.

3.3. Change in Composition of AAC Waste over Time and Chemical Reactions

The accumulation of sulfur in AAC waste is clearly demonstrated by the increase in the sulfur content of the material, measured using the energy dispersive X-ray Fluorescence spectrometer (Figure 4). The transformation of the material is due to chemical reactions between AAC waste and H_2S under humid conditions, resulting in a change in the mechanical structure of the material [21], observable through pressure drops in the PBR. From XRD analysis, Poser et al. [14] demonstrated that the primary reaction between H_2SO_4 (resulting from the oxidation of H_2S as indicated hereafter) and AAC waste leads to the consumption of calcium oxides and the formation of calcium sulfate ($CaSO_4 \cdot 2H_2O$, i.e., gypsum), as shown in Equations (1)–(4).

$$\text{Tobermorite: } Ca_5Si_6O_{16}(OH)_2\ 4H_2O + 5H_2SO_4 \rightarrow 5CaSO_4\ 2H_2O + 6SiO_2 + 4H_2O, \quad (1)$$

$$\text{Calcium carbonate: } CaCO_3 + H_2SO_4 + 2H_2O \rightarrow CaSO_4\ 2H_2O + CO_2, \quad (2)$$

$$\text{Calcium hydroxide: } Ca(OH)_2 + H_2SO_4 \rightarrow CaSO_4\ 2H_2O, \quad (3)$$

$$\text{Calcium-Silicate-Hydrate: } 3CaO\ 2SiO_2\ nH_2O + 3H_2SO_4 \rightarrow 3CaSO_4\ 2H_2O + 2SiO_2 + mH_2O, \quad (4)$$

The formation of gypsum is confirmed through Scanning Electron Microscopy (SEM) coupled with energy-dispersive X-ray spectroscopy, as illustrated in Figure 5. As indicated by Equations (1)–(4), gypsum formation results from the acid attack of calcium oxides by H_2SO_4 [11]. Sulfuric acid may form via the oxidation of H_2S in an aqueous environment (Equation (5)) or through the reaction of SO_3, which is present in substantial amounts in AAC waste, with water (Equation (6)). The direct oxidation of H_2S with O_2 in the gas is also possible (Equation (7)), and elemental sulfur (S^0) may further convert into sulfate (SO_4^{2-}) in the presence of excess oxygen. Additionally, sulfur removal may occur through the reaction between iron(III) oxide in AAC waste and H_2S, forming iron(II) sulfide (Equation (8)). In the presence of oxygen, iron(II) sulfide can further react, regenerating iron(III) oxide (Equation (9)), as detailed by [22].

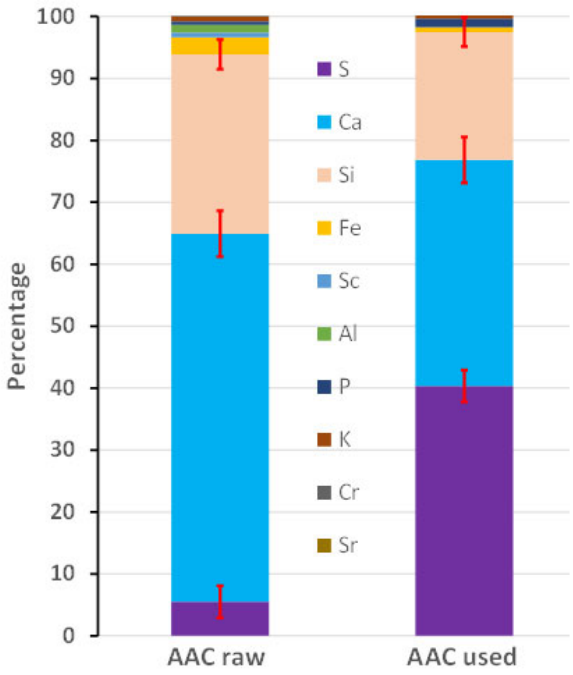


Figure 4. Change in the composition of AAC between the start (AAC raw) and the end (AAC used) of experiment (mass percentage).

$$H_2S + 2O_2 \rightarrow H_2SO_4, \quad (5)$$

$$SO_3 + H_2O \rightarrow H_2SO_4, \quad (6)$$

$$H_2S + 0.5O_2 \rightarrow S^0 + H_2O, \quad (7)$$

$$H_2S + 2Fe^{3+} + 2OH^- \rightarrow 2Fe^{2+} + 2H_2O + S^0, \quad (8)$$

$$2Fe^{2+} + H_2O + 0.5O_2 \rightarrow 2Fe^{3+} + 2OH^-, \quad (9)$$

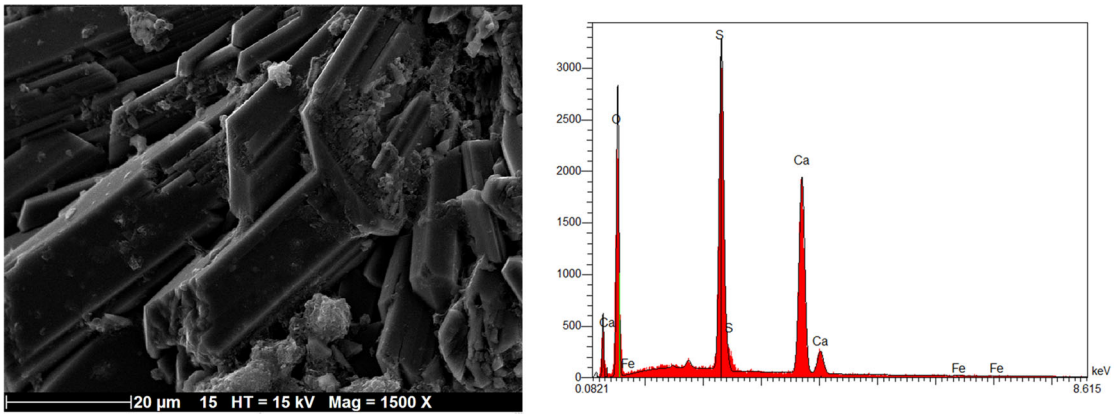


Figure 5. Identification of gypsum presence. Left: example of SEM image of AAC sample recovered from the PBR. Right: chemical characterization from energy-dispersive X-ray spectroscopy.

According to the stoichiometry of Equation (5), 2 moles of oxygen are required to remove 1 mole of H_2S, whereas Equation (7) requires only 0.5 moles of oxygen per mole of H_2S. Similarly, the reaction of H_2S with iron(III) oxide (Equations (8) and (9)) also consumes 0.5 moles of oxygen per mole of H_2S to regenerate Fe_2O_3. Consequently, H_2S removal is accompanied by oxygen consumption. Oxygen consumption was monitored between days 50 and 89 of the experiment under steady-state conditions, with constant

H_2S and O_2 concentrations in the gas entering the PBR (Figure 6). Between days 50 and 70, the O_2/H_2S ratio fluctuated between 1.5 ± 0.2 and 2.5 ± 0.2. After day 70, a clear downward trend was observed, approaching 0.5 ± 0.2 by the end of the experiment. This evolution correlates with a change in H_2S removal efficiency (Figure 3). Between days 50 and 70, when H_2S removal efficiencies were close to 100%, it is likely that all reactions occurred simultaneously, including gypsum formation, direct oxidation of H_2S to elemental sulfur (S^0), and FeS formation. The presence of elemental sulfur (S^0) and iron sulfide (FeS), visible on the material surface as a yellow deposit and a black coloration (as shown in the top left of Figure 1, i.e., AAC used material), was confirmed by scanning electron microscopy (SEM) coupled with energy-dispersive X-ray spectroscopy. However, after day 70, gypsum formation reactions became less frequent, leading to a simultaneous decrease in H_2S removal efficiency and O_2 consumption. By the end of the experiment, removal efficiencies of 20–30% can be attributed to mechanisms described by Equations (7) and (8), which require 0.5 moles of O_2 per mole of H_2S. In other words, the acid attack of calcium oxides by H_2SO_4 is the dominant mechanism in H_2S removal, achieving near 100% efficiency, whereas reactions involving Fe_2O_3 play a secondary role with limited effectiveness.

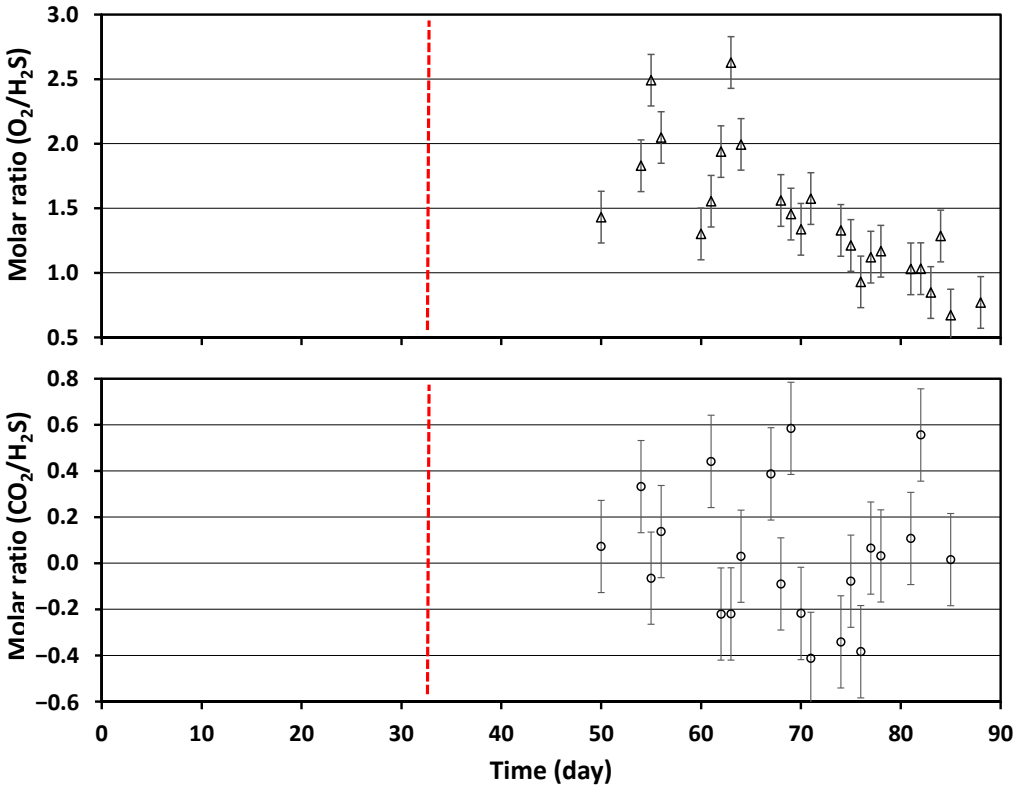


Figure 6. Evolution of the molar ratios O_2/H_2S (top) and CO_2/H_2S (bottom) measured under steady-state conditions of inlet concentrations (H_2S, O_2 and CO_2) in the PBR.

The influence of CO_2 was also monitored between days 50 and 89 of the experiment (Figure 6). Unlike oxygen, no clear conclusion can be drawn regarding CO_2 production or consumption, as the CO_2/H_2S ratio fluctuated between −0.4 ± 0.2 and +0.6 ± 0.2 during this phase of the experiment. Thus, CO_2 is unlikely to participate in reactions between AAC waste and H_2S. In other words, AAC waste does not seem suitable for reducing CO_2 levels in biogas.

3.4. Lifespan of AAC Waste

During the period of near 100% efficiency (between days 54 and 78), the daily H_2S removal capacity of the material remained constant at 4.0 ± 0.2 g_{H_2S} kg_{AAC}^{-1} day^{-1} (Figure 3), which provides a good indication of the potential lifespan of the material under optimal pH and O_2 concentration conditions. For the applied load of 72 ± 4 g_{H_2S} m^{-3} h^{-1}, this lifespan would be 46 days for RE→100% (i.e., 185 g_{H_2S} kg_{AAC}^{-1} divided by 4.0 g_{H_2S} kg_{AAC}^{-1} day^{-1}). This value can be compared with the estimated lifetime determined by [14] the following:

$$t = \frac{\rho_{AAC}}{RC} \%CaO \frac{M_{H_2S}}{M_{CaO}}, \quad (10)$$

With t representing the lifespan of the AAC waste (in h), ρ_{AAC} the AAC bed density ($Mass_{AAC}/V_{AAC}$, in kg m^{-3}), the removal capacity (RC) is defined as the mass of H_2S removed per unit volume of the PBR and per unit of time (in kg_{H_2S} m^{-3} h^{-1}). The removal capacity equals the loading rate when RE = 100%. %CaO is the fraction of calcium oxides constituting the material, and M_{H_2S} and M_{CaO} are the molar masses of H_2S and calcium oxides, respectively (in kg mol^{-1}). The time calculated according to Equation (10), with ρ_{AAC} = 410 kg m^{-3} (derived from the mass of dry AAC waste introduced in the PBR, i.e., 3.2 kg), CaO = 0.246 and RC = 0.072 kg_{H_2S} m^{-3} h^{-1}, underestimates the material's lifespan (36 days). However, Poser et al. [14] noted that this equation considers only the reaction of calcium oxides with H_2S, whereas other elements present in the material may also react, as indicated above. Furthermore, these authors highlighted significant uncertainty in determining the parameter ρ_{AAC}, as the mass of the dry AAC waste introduced at the start of the experiment will have to be reconsidered upwards due to the addition of water and the progressive accumulation of sulfur in the material over time. Consequently, without precise knowledge of the density of the wetted material bed, Equation (10) can only provide a rough estimate of the material's lifetime.

3.5. Packed Bed Reactor Design and Operation Strategies for a Large Scale Biogas Purification

Measurements of H_2S removal efficiency and pressure drops showed that AAC waste can be efficiently and cost-effectively used to remove H_2S from gases, provided that the material is sprayed with highly acidic water and that gases contain some oxygen. However, the relatively short lifetime of the material, due to its high H_2S removal capacity, means that a system with two parallel reactors filled with AAC waste should be designed for industrial-scale treatment of large biogas flows. While one reactor operates, the other undergoes material replacement. Once replaced, the material could be repurposed either for plasterboard production or as a soil amendment [17,23]. The recyclability of AAC waste, transformed into gypsum through reaction with H_2S for potential use as a soil amendment, appears to be the most promising avenue. However, this possibility must be investigated through dedicated studies, including toxicological assessments, to confirm its safety and feasibility. The switching of operation from one reactor to the other will be controlled by monitoring the pressure drops in the operating reactor. However, this operating strategy requires controlling the switch from one reactor to the other to maintain effective H_2S treatment.

A short additional experiment was therefore carried out to verify whether AAC waste are capable of reacting very quickly and effectively with H_2S under optimum operating conditions. The PBR was emptied, and new raw AAC pieces were introduced. These pieces were then sprayed with acidic water at pH = 3.0 ± 0.1 and subjected to the same gas flow used at the end of the previous experiment (i.e., residence time = 22 ± 1 s, H_2S concentration = 420 ± 20 mg $m^{-3,}$ and oxygen concentration around 0.30 ± 0.01%). The results showed that H_2S removal efficiency reached 100% within a few days (less than

one week), demonstrating that the transient period was considerably reduced compared to that observed in the long-term experiment (Figure 1). Then, RE remained constant at 100% during the remainder of the experiment (10 days), with a removal capacity of 70 ± 4 g m^{-3} h^{-1}. The pH decreased slightly to 2.2 ± 0.1, while the oxygen concentration varied between 0.3 and 0.7% (3000–7000 $\pm$ 100 ppm). Consequently, the continuous irrigation of raw AAC waste with highly acidic water ensures high efficiency in H_2S removal, demonstrating the feasibility of large-scale biogas purification using AAC waste.

3.6. Advantages and Drawbacks of Using AAC Waste for H_2S Removal in Biogas

Compared to conventional adsorbent materials, the treatment performance of AAC waste is superior to that of zeolites (40 g_{H_2S} kg^{-1}) and metal-organic frameworks (MOFs) (130 g_{H_2S} kg^{-1}), and comparable to that of activated carbons and biochars (50–200 g_{H_2S} kg^{-1}) [9,24]. However, certain impregnated or doped activated carbons can reach adsorption capacities as high as 850 g_{H_2S} kg^{-1} when treating synthetic biogas in which nitrogen replaces methane [9]. Nevertheless, these functionalized activated carbons are highly expensive, whereas the low cost of AAC waste (on the order of a few tens of euros per ton) clearly positions such waste as a viable alternative to activated carbons, even though some activated carbons can be partially regenerated at high cost. It is also important to note that studies conducted on real biogas streams containing CH_4, CO_2, and H_2S have shown that the adsorption capacities of biochars, zeolites, and activated carbons are significantly lower than those obtained using N_2 as the carrier gas (<70 g_{H_2S} kg^{-1}). However, adsorption capacities of 383 g_{H_2S} kg^{-1} and up to 1266 g_{H_2S} kg^{-1} have been reported in the literature. It is therefore essential to assess the performance of AAC waste in the treatment of real biogas in order to enable accurate comparisons.

Regarding end-of-life considerations for materials, activated carbons and AAC waste can be compared in terms of their respective disposal routes. On the one hand, the incineration of activated carbons requires specialized facilities capable of treating emitted gases, while landfilling presents notable environmental constraints. On the other hand, AAC waste offers the advantage of transforming upon contact with H_2S into a new material that can be potentially valorized as a soil amendment. The main limitation in the use of the resulting gypsum lies in the origin of the AAC waste, specifically its initial composition, and in particular the presence of potentially toxic metallic compounds. The composition of AAC waste varies depending on the waste source and its degree of association with other demolition materials. With respect to available waste streams, in Germany, for example, AAC waste generation was estimated at 1.2 million tons in 2020, with projections exceeding 4 million tons by 2050 [25]. These volumes would be more than sufficient to meet the country's biogas treatment needs. Assuming a treatment capacity of 185 g_{H_2S} kg^{-1}, the amount of AAC waste required annually to treat the biogas output of a digester producing 150 Nm^3 h^{-1} with an H_2S concentration of 1000 ppmv (1400 mg m^{-3}) is approximately 10 tons per year. The available AAC waste quantities are thus more than adequate to support large-scale H_2S removal. Nonetheless, attention should be given to sourcing AAC waste locally, in order to minimize transportation needs, both for the supply of fresh material and for the removal of the AAC waste transformed into gypsum byproduct.

The pressure drops generated during filtration using randomly AAC waste also highlight the advantages of this material over activated carbons. The centimeter-scale particle size of AAC waste results in pressure drops of only a few pascals per meter (Figure 3), which are significantly lower than those typically observed in packed beds of powdered or granular activated carbon [26].

Moreover, the removal of H_2S from biogas using AAC waste offers the advantage of being compatible with humid conditions and the presence of oxygen, factors that can

negatively affect the performance of activated carbons. The simultaneous removal of both oxygen and H_2S by AAC waste, following a 2:1 stoichiometric ratio, can be particularly beneficial in anaerobic digesters employing micro-oxygenation to reduce H_2S concentrations in the digester headspace [27,28]. By controlling the amount of air introduced during micro-oxygenation, it may be possible to regulate the O_2/H_2S ratio in order to optimize H_2S removal by AAC waste, ultimately yielding a biogas stream that is free of both H_2S and residual oxygen after treatment.

4. Conclusions

This study demonstrated the effectiveness of AAC waste as a material for removing H_2S from gas streams under specific operating conditions. By maintaining a highly acidic environment and ensuring the presence of oxygen at low concentrations (<1%), AAC waste exhibited H_2S removal efficiencies close to 100% for moderated H_2S concentrations (300 ppm, i.e., 420 ± 20 mg m^{-3}). The transformation of AAC waste, mainly into gypsum, indicated a progressive consumption of the calcium oxides of the material, thereby determining its operational lifespan. This study also highlighted the importance of monitoring pressure drops (ΔP) as a reliable and cost-effective indicator for determining the end of AAC's functional lifespan.

Based on these results, an industrial H_2S treatment system can be designed using two parallel reactors filled with AAC waste. While one reactor is in operation, the other undergoes material replacement. Although the use of AAC waste has not yet been considered by the industry for H_2S treatment in gases such as biogas, the significant recyclability potential of this waste as gas filtration material is evident, offering a promising alternative to the use of expensive adsorbents in terms of H_2S separation capacity. Thus, the use of AAC waste for H_2S removal in biogas could fit into a dual circular economy approach, contributing to energy transition goals by reducing greenhouse gas emissions and establishing a value chain for AAC waste.

The next steps of this work will involve confirming the obtained performance, as well as the durability of AAC waste, for the treatment of real biogas produced under industrial conditions. Furthermore, the recyclability of AAC waste transformed into gypsum, notably as a soil amendment, will also be studied.

Author Contributions: Conceptualization, E.D. and A.C.; methodology, E.D. and N.K.; software, N.K.; validation, E.D. and A.C.; formal analysis, E.D. and N.K.; investigation, E.D. and N.K.; data curation, E.D. and N.K.; writing—original draft preparation, E.D.; writing—review and editing, E.D. and A.C.; supervision, E.D. and A.C.; project administration, E.D. and A.C.; funding acquisition, E.D. and A.C. All authors have read and agreed to the published version of the manuscript.

Funding: The authors would like to thank GRDF (Gaz Réseau Distribution France, France's leading natural gas distribution operator) for financial support. Also, special thanks to Toinou FREZOULS from GRDF for its continuous support in the process management. The authors would also like to thank Ecominero (www.ecominero.fr) for providing autoclaved aerated concrete waste.

Data Availability Statement: Data is contained within the article.

Acknowledgments: The authors would like to thank the Département Systèmes Energétiques et Environnement of IMT Atlantique (Nantes, France). Also, special thanks to Yvan GOURIOU and Eric CHEVREL for their continuous support in the process management.

Conflicts of Interest: The authors declare no conflicts of interest.

References

1. Zhou, Q.; Wang, W.; Noguchi, T. Recyclable Calcium Carbonate-Based Concrete: Utilizing Calcium Carbonate to Bond Recycled Concrete Fines through an in-Situ Heterogeneous Dual-Precipitation Approach. *Cem. Concr. Res.* **2024**, *186*, 107679. [CrossRef]
2. Olsson, J.A.; Miller, S.A.; Kneifel, J.D. A Review of Current Practice for Life Cycle Assessment of Cement and Concrete. *Resour. Conserv. Recycl.* **2024**, *206*, 107619. [CrossRef]
3. Van Damme, H. Concrete Material Science: Past, Present, and Future Innovations. *Cem. Concr. Res.* **2018**, *112*, 5–24. [CrossRef]
4. Volk, R.; Steins, J.J.; Kreft, O.; Schultmann, F. Life Cycle Assessment of Post-Demolition Autoclaved Aerated Concrete (AAC) Recycling Options. *Resour. Conserv. Recycl.* **2023**, *188*, 106716. [CrossRef]
5. Liu, X.; Wang, M.; Zhang, X.; Liang, T. A New Insight: Investigating Calcium Silicate Hydrate as a Potential Adsorbent for Hydrogen Sulfide Removal. *Surf. Interfaces* **2025**, *56*, 105669. [CrossRef]
6. Calbry-Muzyka, A.; Madi, H.; Rüsch-Pfund, F.; Gandiglio, M.; Biollaz, S. Biogas Composition from Agricultural Sources and Organic Fraction of Municipal Solid Waste. *Renew. Energy* **2022**, *181*, 1000–1007. [CrossRef]
7. Thirumalaivasan, N.; Nangan, S.; Kanagaraj, K.; Rajendran, S. Assessment of Sustainability and Environmental Impacts of Renewable Energies: Focusing on Biogas and Biohydrogen (Biofuels) Production. *Process Saf. Environ. Prot.* **2024**, *189*, 467–485. [CrossRef]
8. Pudi, A.; Rezaei, M.; Signorini, V.; Andersson, M.P.; Baschetti, M.G.; Mansouri, S.S. Hydrogen Sulfide Capture and Removal Technologies: A Comprehensive Review of Recent Developments and Emerging Trends. *Sep. Purif. Technol.* **2022**, *298*, 121448. [CrossRef]
9. Paz, L.; Gentil, S.; Fierro, V.; Celzard, A. Activated Carbons Outperform Other Sorbents for Biogas Desulfurization. *Chem. Eng. J.* **2025**, *506*, 160304. [CrossRef]
10. Jensen, H.S.; Lens, P.N.L.; Nielsen, J.L.; Bester, K.; Nielsen, A.H.; Hvitved-Jacobsen, T.; Vollertsen, J. Growth Kinetics of Hydrogen Sulfide Oxidizing Bacteria in Corroded Concrete from Sewers. *J. Hazard. Mater.* **2011**, *189*, 685–691. [CrossRef]
11. Pramanik, S.K.; Bhuiyan, M.; Robert, D.; Roychand, R.; Gao, L.; Cole, I.; Pramanik, B.K. Bio-Corrosion in Concrete Sewer Systems: Mechanisms and Mitigation Strategies. *Sci. Total Environ.* **2024**, *921*, 171231. [CrossRef] [PubMed]
12. Rozière, E.; Loukili, A.; El Hachem, R.; Grondin, F. Durability of Concrete Exposed to Leaching and External Sulphate Attacks. *Cem. Concr. Res.* **2009**, *39*, 1188–1198. [CrossRef]
13. Mohammadi, K.; Vaiskunaite, R.; Zagorskis, A. Innovative Biofiltration Materials for H2S Removal from Biogas. *Environ. Health Eng. Manag. J.* **2024**, *11*, 361–370. [CrossRef]
14. Poser, M.; Duarte E Silva, L.R.; Peu, P.; Couvert, A.; Dumont, É. Cellular Concrete Waste: An Efficient New Way for H2S Removal. *Sep. Purif. Technol.* **2023**, *309*, 123014. [CrossRef]
15. Germain, C.; Poser, M.; Peu, P.; Couvert, A.; Dumont, E. Hybrid Filtration Process for Gas Desulfurization. *Processes* **2023**, *11*, 3438. [CrossRef]
16. Mohammadi, K.; Vaiškūnaitė, R.; Zigmontienė, A. Efficiency of Hydrogen Sulfide Removal from Biogas Using a Laboratory-Scale Biofilter Packed with Biochar, Cellular Concrete Waste, or Polyurethane Foam: A COMSOL Simulation Study. *Processes* **2025**, *13*, 329. [CrossRef]
17. Liu, S.; Liu, W.; Jiao, F.; Qin, W.; Yang, C. Production and Resource Utilization of Flue Gas Desulfurized Gypsum in China—A Review. *Environ. Pollut.* **2021**, *288*, 117799. [CrossRef] [PubMed]
18. Gasquet, V.; Kim, B.; Bonhomme, A.; Benbelkacem, H. Sewage Sludge Ash-Derived Materials for H2S Removal from a Landfill Biogas. *Waste Manag.* **2021**, *136*, 230–237. [CrossRef]
19. Golmakani, A.; Ali Nabavi, S.; Wadi, B.; Manovic, V. Advances, Challenges, and Perspectives of Biogas Cleaning, Upgrading, and Utilisation. *Fuel* **2022**, *317*, 123085. [CrossRef]
20. Pipatmanomai, S.; Kaewluan, S.; Vitidsant, T. Economic Assessment of Biogas-to-Electricity Generation System with H2S Removal by Activated Carbon in Small Pig Farm. *Appl. Energy* **2009**, *86*, 669–674. [CrossRef]
21. Anwar, A.; Liu, X.; Zhang, L. Biogenic Corrosion of Cementitious Composite in Wastewater Sewerage System–A Review. *Process Saf. Environ. Prot.* **2022**, *165*, 545–585. [CrossRef]
22. Dumont, E. H_2S Removal from Biogas Using Bioreactors: A Review. *Int. J. Energy Environ.* **2015**, *6*, 479–498.
23. Wang, J.; Yang, P. Potential Flue Gas Desulfurization Gypsum Utilization in Agriculture: A Comprehensive Review. *Renew. Sustain. Energy Rev.* **2018**, *82*, 1969–1978. [CrossRef]
24. Gao, X.; Xiao, Z.; Wu, P.; Liu, Y.; Xu, H.; Wang, Y. Recent Research Advances in Adsorption Removal of Gaseous Hydrogen Sulfide by Biochar. *Fuel* **2025**, *388*, 134390. [CrossRef]
25. Steins, J.J.; Volk, R.; Schultmann, F. Modelling and Predicting the Generation of Post-Demolition Autoclaved Aerated Concrete (AAC) Volumes in Germany until 2050. *Resour. Conserv. Recycl.* **2021**, *171*, 105504. [CrossRef]
26. Hassan, E.B.E.; Hoffmann, J. Review on Pressure Drop through a Randomly Packed Bed of Crushed Rocks. *Discov. Appl. Sci.* **2024**, *6*, 126. [CrossRef]

27. Muller, C.; Guevarra, K.; Summers, A.; Pierce, L.; Shahbaz, P.; Zemke, P.E.; Woodland, K.; Hollingsworth, V.; Nakhla, G.; Bell, K.; et al. A Review of the Practical Application of Micro-Aeration and Oxygenation for Hydrogen Sulfide Management in Anaerobic Digesters. *Process Saf. Environ. Prot.* **2022**, *165*, 126–137. [CrossRef]
28. Khadir, A.; Nakhla, G.; Karki, R.; Raskin, L.; Muller, C.; Guevarra, K.; Summers, A.; Pierce, L.; Shahbaz, P.; Bell, K.; et al. Micro-Aeration for Hydrogen Sulfide Reduction in Full-Scale Anaerobic Digesters with Limited Headspace: Performance and Sulfide Reduction Kinetics. *Process Saf. Environ. Prot.* **2025**, *196*, 106911. [CrossRef]

Disclaimer/Publisher's Note: The statements, opinions and data contained in all publications are solely those of the individual author(s) and contributor(s) and not of MDPI and/or the editor(s). MDPI and/or the editor(s) disclaim responsibility for any injury to people or property resulting from any ideas, methods, instructions or products referred to in the content.